Comparative structure-function studies of chickpea and durum wheat uncover mechanisms by which cell wall properties influence starch bioaccessibility

Cathrina H. Edwards[1,2¥*], Peter Ryden[2], Giuseppina Mandalari[2,3], Peter J. Butterworth[1], Peter R. Ellis[1*]

[1] Biopolymers Group, Departments of Biochemistry and Nutritional Sciences, Faculty of Life Sciences and Medicine, King's College London, SE1 9NH, London, UK

[2] Quadram Institute Bioscience, Norwich Research Park, NR4 7UQ, Norwich, UK

[3] Department of Chemical, Biological, Pharmaceutical and Environmental Science, University of Messina, Vill. SS. Annunziata, 98168, Messina, Italy

[¥]Current address: Quadram Institute Bioscience, Norwich Research Park, NR4 7UQ, Norwich, UK.

E-mail: cathrina.edwards@quadram.ac.uk; peter.ryden@quadram.ac.uk; gmandalari@unime.it; peter.butterworth@kcl.ac.uk; peter.r.ellis@kcl.ac.uk

*CORRESPONDING AUTHOR: Prof. Peter R. Ellis

E-mail: peter.r.ellis@kcl.ac.uk; Tel: +44 (0) 207 848 4238; Fax: +44 (0) 207 848 4328;

Mailing address: Biopolymers Group, Departments of Biochemistry and Nutritional Sciences Division, King's College London, Franklin-Wilkins Building, 150 Stamford Street, SE1 9NH, London, UK

Abstract

Positive health effects of dietary fibre have been established; however, the underpinning mechanisms are not well understood. Plant cell walls are the predominant source of fibre in the diet. They encapsulate intracellular starch and delay digestive enzyme ingress, but food processing can disrupt the structure. Here we compare digestion kinetics of chickpea (cotyledon) and durum wheat (endosperm), which have contrasting cell wall structures (Type I and II, respectively), to investigate a 'cell-wall barrier' mechanism that may underpin the health effects of dietary fibre. Using *in vitro* models, including the Dynamic Gastric Model, to simulate human digestion together with microscopy, we show that starch bioaccessibility is limited from intact plant cells and that processing treatments can have different effects on cell integrity and digestion kinetics when applied to tissues with contrasting cell wall properties. This new understanding of dietary fibre structure is important for effective fibre supplementation to benefit human health.

Introduction

The long-term health benefits of dietary fibre include risk reduction and improved management of cardiometabolic diseases[1], yet the physiological mechanisms underpinning them are not fully understood. Terminology describing fibre in health relates to its solubility and/or composition, but the structure and properties of fibre as cell wall bioassemblies that encapsulate macronutrients have received much less attention [2]. Here, we consider mechanisms by which fibre influences starch bioaccessibility by comparing two widely consumed starch-staple crops with contrasting cell wall structures, chickpea (*Cicer arietinum* L.) and durum wheat *(Triticum durum* L.). Chickpeas, beans and other dicotyledonous plant seeds have Type I cell walls, rich in pectic polysaccharides and xyloglucans; wheat and other monocotyledonous cereal grains have Type II primary cell walls, low in pectin, but rich in arabinoxylans and/or mixed-linkage (1→3),(1→4)-β-D-glucans [3].

In studies of pulses, cellular integrity is a critical factor underpinning their low glycaemic index [4]. The tendency of leguminous cells to separate is commonly observed in hydrothermally-processed chickpeas and many other pulses, but not in beans that exhibit hard-to-cook defects [5]. Cell separation is possible in tissues where the middle lamella is held together largely by non-covalent crosslinking (i.e. pectic polysaccharides) and results from solubilisation and/or heat-catalysed depolymerisation of pectin in the middle lamella of contiguous cells under certain processing conditions [3]. This weakening of inter-cellular adhesions means that hydrothermally-treated legume cotyledon cells can separate from each other during mastication. The resulting intact cells that constitute the food bolus can therefore be the main structural entity that enters the gastrointestinal tract (GIT) [6]. Micrographs of intact, starch-containing plant cells from white haricot beans and mature peas in human ileal fluid [7,8] confirm that cellular structures from leguminous plant tissues with Type I cell walls persist to some extent in the upper GIT. In contrast, wheat endosperm tissues have Type II cell walls and do not cell separate when hydrothermally-processed. Wheat grains fracture following mechanical processing such that the proportion of starch

63 that remains encapsulated within plant cells is likely to depend on the cell volume and
64 particle size of the wheat tissue [9]. Although wheat is conventionally dry-milled to a sub-
65 cellular flour prior to cooking and consumption, we previously showed that large
66 macroparticles of wheat endosperm tissue can remain intact during transit through the upper
67 GIT, leading to an attenuation of postprandial glycaemia compared with sub-cellular flour [10].

68 Several previous *in vitro* digestibility studies have observed lower starch digestibility
69 associated with intact cells or tissues of cooked legumes [11-14] and cereals [15-17]. One
70 possibility is that the cell walls, which are not digested by mammalian enzymes of the upper
71 GIT, exist as physical barriers to delay enzyme ingress. The degree of penetration of
72 digestive enzymes through cell walls is likely to be influenced by many factors such as cell
73 wall thickness, density and composition, and the size and number of cell wall pores
74 including plasmodesmata as well as processing treatments [2,6,18]. Assessing the permeability
75 of cereal endosperm cells, which can remain intact within food macroparticles, is difficult, but
76 indirect microscopic evidence suggests that amylase can cross the cell wall [10]. An additional
77 mechanism of interest is the proposed role of the cell wall in limiting starch gelatinisation
78 and thereby starch susceptibility to amylase digestion [19]. Observations of distorted granular
79 swelling [11] and quantitative studies showing limited gelatinisation of starch [19] within legume
80 tissues provides evidence for this mechanism; however, it is unclear whether this can be
81 rate limiting.

82 Through a series of comparative structure-function studies of chickpea and wheat, we
83 elucidate the mechanisms by which cell wall properties influence starch bioaccessibility. The
84 proposed role of encapsulating cell walls in impeding intracellular starch gelatinisation
85 and/or enzyme access was examined in digestibility studies supplemented with microscopy
86 of samples taken before and after processing and digestion. The Dynamic Gastric Model
87 (DGM) in combination with the Static Duodenal Model (SDM) were used to provide a
88 physiologically-relevant simulation of the human stomach and duodenum, respectively [20,21].
89 Deeper insight of the properties of these different cell wall types, particularly their behaviour

during processing and digestion, can improve our understanding of the mechanisms by which different sources of dietary fibre influence public health. Also, this could lead to the development of more effective and palatable forms of dietary fibre for improving glucose homeostasis in individuals with or at risk to type 2 diabetes.

Results

A series of *in vitro* digestibility studies provided new insight into mechanisms by which plant tissue structure influences starch bioaccessibility from chickpea cotyledon and durum wheat endosperm.

Lower digestibility of cell wall encapsulated starch.

Chickpea and durum wheat were dry-milled to obtain different size fractions and then hydrothermally-processed to inactivate endogenous amylase prior to determination of starch digestibility **(Figure 1).** The larger particles, which contained more cell wall encapsulated starch, had the lowest starch digestibility. As the cellular integrity of the tissue was further disrupted through reductions in particle size, both the rate and proportion of starch digested by amylase increased. In chickpea materials **(Fig. 1a)**, particle size, and thereby cell wall encapsulation of starch, limited the extent of starch digestion (mean percentage digested with standard error after 220 min was 82.5 ± 1.5%, 82.9 ± 0.3%, 65.9 ± 2.0%, 57.0 ± 2.2%, and 33.0 ± 0.9% for starch, and particle size fractions <0.21, 0.38, 0.55 and 1.85 mm, respectively), and plateaued within 60 min of amylolysis. In durum wheat, differences in digestion rate were evident, but the extent of starch digested after 230 min (around 80%) was similar for all durum wheat size fractions, except the largest 1.85 mm fraction, where 66 ± 2.7% of the starch had been digested and had not yet reached a plateau (**Fig. 1b)**. These differences suggest that chickpea cell walls hinder amylase access to a greater extent than do cell walls of wheat. The starch digestibility profiles of boiled starch extracted from chickpea and wheat were similar, thus confirming that the kinetic effects are attributed to properties of the cellular tissue, rather than the starch structure.

Cell integrity after homogenisation limits starch digestibility.

We investigated how the two plant tissues behave after hydrothermal cooking (100°C) when subjected to high shear, and the extent to which this influences starch digestibility and tissue microstructure. The largest of the wheat and chickpea macroparticles (1.85 mm) prepared by dry-milling, and containing the highest proportion of encapsulated starch, were prepared as a porridge and homogenised or left intact prior to the starch amylolysis assay.

Micrographs show the internal structural integrity of intact chickpea (**Fig. 2a**) and durum wheat (**Fig. 2b**) macroparticles after they have been cooked but not homogenised. The chickpea and wheat tissues were comprised of predominantly intact starch-rich cells of cotyledon and endosperm tissues respectively, with some ruptured cells evident at the particle edges (**Fig. 2ab**). Chickpea cotyledon cells had thicker walls (~1 - 2 μm, estimated from micrographs) than wheat endosperm cell walls (≤1 μm) and a rounded appearance, consistent with solubilisation of middle lamellar pectin and weakening of cell-cell adhesion during hydrothermal processing. Durum wheat endosperm cell walls were visibly thinner and less defined (~0.6 - 1 μm, estimated from micrographs), and the endosperm cells were more angular and tightly associated. After 2 h of *in vitro* digestion, chickpea cells at the particle edge and core appeared intact, with starch enclosed (**Fig. 2c**), whereas starch-containing cells of durum wheat endosperm were still present at the particle core (**Fig. 2d).** After 6 h of *in vitro* digestion, the overall structural integrity of the 'intact' chickpea macroparticles remained largely unchanged (**Fig. 2e**). Wheat endosperm cells near the particle edge were ruptured and starch from the cells is presumed to be digested (**Fig. 2f)**. Wheat endosperm cells near the particle core were intact and the amount of intracellular starch granules appeared to be reduced in the outermost cell layers, although the quantitative data in **Fig. 3** provides a more reliable indication of starch digestion.

The effect of homogenisation on tissue structures and starch digestibility is shown in **Figure 3.** The micrographs reveal that when homogenisation treatment was applied to intact macroparticles of hydrothermally-processed chickpea cotyledon (**Fig. 3a)**, the tissue

became disrupted and individual cells had separated, with only a few cells showing evidence of structural damage or cell wall rupture. Most of the cotyledon cells remained intact with the starch encapsulated by the cell walls. When the same homogenisation treatment was applied to the macroparticles of hydrothermally-cooked intact wheat endosperm, it caused extensive cell and tissue structure damage, exposing partially swollen starch granules and other intracellular debris (**Fig. 3b**). No intact endosperm cells or tissue clusters were detected in these wheat samples, only protein fragments and some bran residue (i.e. the pericarp, testa and aleurone layers) against a background of mostly swollen starch granules. In micrographs taken after 6 h digestion with amylase, intact chickpea cells remained **(Fig. 3c)** and had a similar appearance to the cells in the sample collected before digestion, whereas the free starch from ruptured cells appeared to have been digested. In the image of the homogenised and digested wheat endosperm, there was little evidence of any starch remaining, at least not in the form of identifiable starch granules (**Fig. 3d)**.

Starch digestibility curves showing digestion of hydrothermally-cooked chickpea and wheat macroparticles that had been homogenised compared with structurally-intact (non-homogenised) controls are shown in **Figure 3e and f**. Homogenisation of chickpea materials produced a significant increase in the extent of starch digestion, but the intact chickpea samples showed persistently lower levels of digestion even after 6 h incubation (**Fig. 3e**). Similarly, homogenisation of cooked durum wheat macroparticles led to a significant increase in the rate of starch digestion (**Fig. 3f**); however, the same amount of starch (approximately 50%) had been digested after 6 h in both the intact and homogenised wheat samples.

Structure regulates starch bioaccessibility in the stomach and duodenum.

The purpose of these experiments was to study starch bioaccessibility and digestion, and tissue/cell microstructure of chickpeas and durum wheat, prepared as porridge test meals, under simulated physiological conditions of oral, gastric and duodenal digestion. For the chickpea experiments, the main objective was to determine the effects of freeze-milling on

the digestibility and structural integrity of separated chickpea cells. For the wheat experiments, the main objective was to determine the effects of particle size of wheat macroparticles on starch bioaccessibility and digestion, and also monitor microstructural changes.

Chickpea Porridge.

Starch digestion from chickpea porridges with contrasting cellular integrity is shown along with micrographs in **Figure 4.** In the gastric phase, the amount of reducing sugars released from starch by human salivary amylase was minimal, accounting for 1 - 2% of the total starch present in the porridge meals. The concentration of reducing sugars remained constant between 10 and 60 min of gastric incubation, and there was no evidence that starch digestion (by salivary amylase) continued during gastric digestion of either porridge type (**Fig. 4a).**

Once in the duodenal phase, starch amylolysis in the porridge made from freeze-milled chickpea cells progressed rapidly within the first 15 min, whereas amylolysis in the porridge made from intact cells progressed more slowly and to a lesser extent **(Fig. 4b).** For the porridge prepared from intact cells, there was no difference between duodenal digestion profiles of samples that had different gastric residence times, indicating that the gastric phase had no effect on the susceptibility of starch in these porridges to subsequent duodenal amylolysis (***Supplementary Figure 1*****).** However, for porridge made from freeze-milled cells, there was a tendency for samples that had ≤20 min in the gastric phase to be more susceptible to amylolysis during subsequent duodenal digestion (***Supplementary Figure 1*****).**

Progress of total starch amylolysis throughout gastric (60 min) and subsequent duodenal digestion is shown for both porridge types in **Figure 4c.** Starch bioaccessibility from porridge made of intact cells of chickpea cotyledon was very low, with less than ~10% of the starch becoming digested, whereas up to 26% of the starch in the porridge made from

196 freeze-milled cells was digested. For both porridge types, the duodenal phase was the
197 predominant site of starch amylolysis. Micrographs (**Fig. 4d**) revealed that a high proportion
198 of cells remained intact despite the freeze-milling treatment, and that these cellular
199 structures with encapsulated starch remained intact after duodenal digestion.

200 The total amount of starch digested at the end of the duodenal phase for each
201 gastric residence time and porridge type is shown in **Fig. 4e.** The total extent of starch
202 digested was higher from the porridge made with freeze-milled cells than from intact cells.
203 However, the majority of starch in both porridge types remained undigested, with around
204 90% and 75% of starch in the porridges made from intact and freeze-milled cells,
205 respectively, remaining at the end of the duodenal phase. A slight reduction in the total
206 extent of digestion was observed for samples retained in the gastric phase for a longer
207 period. This effect was more pronounced in the porridge made from freeze-milled cells,
208 which could reflect the retention of larger particles (intact cells, which have a lower
209 susceptibility to amylolysis than free starch) in the DGM.

210 *Wheat Porridge.*

211 Starch digestion from wheat porridges made with different particle sizes of endosperm is
212 shown together with micrographs in **Figure 5**. Starch digestion by salivary amylase
213 continued throughout the gastric phase and the gastric starch digestion profiles (**Fig. 5a**)
214 show a similar time-dependent increase in starch amylolysis for all size fractions of wheat
215 used for preparing the porridge. After 60 min in the gastric phase, up to 16% of the total
216 starch in the wheat porridges had been digested. Once in the duodenal phase, starch
217 amylolysis progressed rapidly within the first 4 min and plateaued within 60 min for all size
218 fractions (**Fig. 5b).** Under duodenal conditions (not including the contributions from the
219 gastric phase), on average 48% (range = 34 to 54%) of the total starch in the wheat
220 porridges made from smaller particle size fractions (median size 0.11, 0.38 and 1.01 mm)
221 was digested, whereas an average of 30% (range = 25 to 35%) of the total starch in the
222 larger size fractions (median size 1.44 and 1.95 mm) was digested. There was a general

tendency for samples that had ≤ 20 min of gastric residence to be digested in the duodenal phase more slowly than samples with >20 min of gastric incubation, which suggests that samples with a short gastric residence were less susceptible to subsequent duodenal amylolysis (***Supplementary Figure 2***). Progression of starch amylolysis throughout gastric (60 min) and duodenal digestion are shown in **Fig. 5c,** and it is seen that for all size fractions, gastric starch amylolysis (by residual salivary α-amylase) made some contribution to total amylolysis, but the majority of starch amylolysis occurred within the first 4 min of exposure to pancreatic α-amylase in the duodenal model. On average, the proportion of total starch digestion attributed to the gastric phase was about 19% of the total starch amylolysis (range from 7 – 26 %), where the values at the lower end of this range originate from samples that experienced shorter gastric residence times. The remaining 81% (range from 74 to 93 %) of the total starch amylolysis occurred within the duodenal phase and mostly within the first 4 min (as shown in **Fig. 5c)**. Micrographs (**Fig. 5d**) show that starch had been digested from exposed granules (sizes 0.11 and 1.01 mm) and from the peripheral cells of larger macroparticles (size 1.95 mm) in samples recovered from the duodenal phase. The total amount of starch digested at the end of the duodenal phase for each gastric residence time and particle size is shown in **Fig. 5e**. The total extent of digestion increased with gastric residence time and decreasing particle size.

Discussion

These studies were performed to gain insight into the underlying mechanisms of starch digestion in edible plants, specifically, chickpea cotyledon with Type I primary cell walls, and durum wheat endosperm with Type II cell walls. Identical mechanical treatment (dry-milling, homogenisation) of these tissues had different effects on starch bioaccessibility, with implications for glycaemic responses and the nature and amount of resistant starch that is delivered to the colon. These studies highlight the importance of tissue fracture properties and cell wall permeability as key mechanisms by which ‘dietary fibre’ influences starch bioaccessibility.

In wheat, the final amount of starch digested in different sized fractions was the same, but the time to reach the endpoint was dependent on particle size, whereas in chickpeas, size greatly affected the final amount of starch digested. These results are consistent with predictions from our previous kinetic studies of early stages of digestion of plant material [15].

The marked disparity in digestibility profiles between wheat and chickpeas is likely explained by intrinsic differences in the cell tissue properties, especially the permeability of cell walls to amylase diffusion. Digestion of intracellular starch from wheat endosperm indicates that the cell walls were permeable to α-amylase. In contrast, digestion of starch from chickpea tissue was limited to ruptured cells on the fractured surface of particles, and is consistent with reports of low starch amylolysis from intact leguminous plant cells [11-13,22,23]. Restricted amylolysis is a consequence of a low permeability to amylase ('cell wall barrier mechanism') and/or intracellular starch being less susceptible to amylolysis ('restricted gelatinisation mechanism'). The higher dietary fibre values of chickpea flour reflect their thicker cell walls, which account for ~5-6% of the cotyledon tissue mass, compared with wheat endosperm (flour) which comprises ~2-3% of cell wall material [24].

The relative contributions of these two mechanisms was investigated further in studies where hydrothermally cooked macroparticles were disrupted by homogenisation (blending) treatment. These studies revealed extensive cell fracture in wheat (i.e. the cell wall barrier was removed), and the starch was digested more rapidly than in control samples with intact tissue structure. However, even after 6 h incubation with α-amylase, 50% of the starch in both the intact and homogenised wheat sample remained undigested suggesting that starch cooked inside this plant matrix retained some ordered structure [19]. For chickpeas, the tissue separated into individual cells with intact cell walls so that access to intracellular starch was impeded.

275 The contrasting fracture/separation behaviour of hydrothermally-cooked durum
276 wheat and chickpea tissues has implications for the type of cell wall structures that digestive
277 enzymes are likely to encounter *in vivo*. Under simulated digestive conditions of the stomach
278 and duodenum, chickpea cells remained intact and the bioaccessibility of starch from these
279 cells was very low.

280 In hydrothermally-cooked wheat endosperm, larger particles of tissue remained
281 intact throughout simulated gastric and duodenal digestion with a progressive loss of starch
282 from intact cells near the particle periphery towards the core. This is consistent with
283 digestion patterns observed from large endosperm particles recovered from the terminal
284 ileum of human participants in an *in vivo* study, where reduced bioaccessibility of starch in
285 endosperm macroparticles significantly attenuated postprandial glycaemic and insulinaemic
286 responses [10].

287 The physiological conditions simulated in DGM and SDM digestion models are
288 considered to be more representative than direct amylolysis assays [20,21]. The rate and
289 extent of amylolysis is recognised as being relevant for predictions of glycaemic responses
290 [25,26] but the acidity and mixing of the stomach, and activities of other enzymes (e.g., pepsin
291 and trypsin digestion of proteins) has been suggested to influence subsequent duodenal
292 amylolysis. We observed that salivary amylase (added during the oral phase) continued to
293 digest wheat starch throughout the gastric phase, accounting for ~ 20 % of the total starch
294 amylolysis in wheat, but digested < 2% of the starch from chickpea cells. Thus, the
295 mechanisms by which cell walls affect starch digestibility in the duodenal phase are equally
296 relevant to the oral digestion. Gastric residence in excess of 20 min was associated with a
297 slight change in the rate and extent of subsequent duodenal starch amylolysis (an increase
298 for wheat and decrease for chickpeas). However, no changes in cell wall or tissue structures
299 were evident from the microscopy of samples recovered from the DGM, and it is noteworthy
300 that due to the gastric sieving, this difference could reflect the dissimilar nature of material

301 being released into the duodenal phase. Nevertheless, most of starch digestion from these
302 samples occurred within the early stages of duodenal digestion.

303 From a nutritional perspective, the reductions in the rate and extent of starch
304 bioaccessibility observed in our *in vitro* studies would be expected to produce an attenuation
305 in glycaemic and insulinaemic responses *in vivo*, and the amount of resistant starch
306 remaining at the end of simulated upper gastrointestinal digestion would be available for
307 fermentation by the colonic microbiome. Thus, processing treatments (e.g., combinations of
308 dry-milling, cooking and blending) having different effects on the cellular integrity and cell
309 wall permeability of starch-storage tissues are highly relevant to our understanding of the
310 physiological effects of 'dietary fibre' from legumes and cereals. Such mechanistic
311 understanding has potential for optimising health benefits of 'dietary fibre' components of
312 foods for gastrointestinal health, prevention of type 2 diabetes and weight management. Our
313 studies emphasise the crucial importance of structural integrity of dietary fibre in explaining
314 physiological mechanisms of fibre. The inclusion of the innovative DGM in combination with
315 the SDM has provided a physiologically relevant simulation of the proximal GIT conditions to
316 demonstrate the contrasting behaviour of legume and wheat tissues during digestion. In
317 particular, the DGM, which was employed to mimic both biochemical and mechanical
318 processes of gastric digestion in a realistic time-dependent way, has shown that starch
319 digestion in wheat is enhanced by gastric conditions compared with chickpea tissue. The
320 results raise questions about fibre supplementation and health claims when the physical
321 form of fibre is not retained during food processing. Moreover, this work highlights the
322 problems of relying only on chemical analysis of dietary fibre for characterising the
323 physiological properties of fibre in plant foods, particularly when this information is used to
324 interpret mechanistic data and the results of human studies. Further research on the
325 supramolecular structure, mechanical properties and porosity of cell walls would add to our
326 understanding of the physiological and clinical effects of dietary fibre [2]. Such insight could
327 also help the food industry to design more effective fibre-rich food ingredients and products.

Methods

Materials.

Dried seeds of chickpea, *Cicer arietinum* L. (Russian variety), were donated by Poortman Ltd. Samples of durum wheat, *Triticum durum* L. (Svevo variety), were provided by Millbo S.p.a., Italy. Starch was isolated from these grains, purified and dried as described previously [15] for use as a reference material in some experiments. Milled macroparticles of a defined size were prepared from the starch-rich storage tissue of each species. Chickpeas were soaked overnight and then manually de-hulled while wet to remove the testa, and finally left to dry at ambient temperature until the weight had stabilised and moisture <10% was reached. Durum wheat grains were de-branned for 2 min (Satake TM-05C de-branner equipped with a medium abrasive roller No. 40; roller speed, 1450 rpm) to remove the outer bran layers. The dry chickpea cotyledon and wheat endosperm tissues were then roller-milled (Satake Test Roller Mill ST-100 equipped with 10.5fl/ in break rolls; 250 mm diameter) using a sharp-to-sharp disposition to achieve geometrically well-defined macroparticles. The milled material was separated into particle size fractions as denoted in the following sections by the median size based on sieve apertures.

Proximate analysis.

Proximate analysis (protein, lipid, dietary fibre by AOAC, ash (total mineral content), moisture and carbohydrate by difference) of durum wheat and chickpea materials was done by Rank Hovis Mill Analytical Services (Premier, High Wycombe) as described previously [10]. The total starch content of these materials was measured directly using a modified version of the AOAC 996.11 Total Starch Procedure with Megazyme Total Starch Assay kit reagents (Megazyme International Ireland Ltd.) as described in full elsewhere [10]. Milled chickpea fractions contained 23 g protein, 22.6 g dietary fibre, 5.3 g lipid, 2.8 g ash, 8.7 g moisture, 37.5 g carbohydrate (by difference) per 100 g ‘as is’. Milled durum wheat endosperm contained 10.7 g protein, 6.5 g dietary fibre, 1.7 g lipid, 0.9 g ash, 9.9 g moisture, 70.2 g

carbohydrate (by difference) per 100 g 'as is'. Total starch content of milled size fractions was 40 ± 2 % for chickpea and 63 ± 2 % for durum wheat.

Light microscopy.

Samples for light microscopy were collected before and after digestion procedures. Samples of intact macroparticles were fixed overnight in modified Karnovsky's fixative (1.6%, v/v, formaldehyde, 2%, v/v, glutaraldehyde), rinsed in 0.1 M sodium cacodylate buffer (pH 7.2) and then dehydrated through a graded ethanol series. Samples were embedded in LR-White Resin (62662 Fluka) and polymerised (cured) at 60 ± 2°C for 24 h. Sections (0.5 or 1 µm) were cut using a glass knife mounted on an ultramicrotome (Ultracut E, Reichert-Jung), dried and stained with 1 % (w/v) toluidine blue in 1 % (w/v) sodium borate or Lugol's Iodine (2.5% I_2 with 5% KI). Sections (0.5 - 1 µm) were viewed using a Leica Zeiss Axioskop 2 mot plus light microscope and images captured using a Zeiss AxioCam HRc camera and AuxioVision v3.1 microscope software. Micrographs of homogenised samples were obtained by immediate examination of sections without prior fixation.

Starch amylolysis assay.

The susceptibility of chickpea and wheat materials to starch amylolysis was assayed following a protocol that has been described previously [15]. In brief, 50 mL tubes containing suspensions of materials for testing were incubated in a water bath at 37 °C for 20 min. A blank aliquot (200 µL) of the solution was then removed to a microfuge tube and mixed with an equal volume of ice-cold 0.3 mol/L Na_2CO_3 ('stop solution'). To start the amylolysis reaction, porcine-pancreatic amylase (prepared in PBS from high purity enzyme A6255 obtained from Sigma-Aldrich Co Ltd, Poole Dorset; EC 3.2.1.1) was immediately added to the suspensions, to achieve a ratio of 2.3 nmol/L amylase (~0.17 U) per mg starch in the final digestion mixture. The sample tubes were incubated on a rotary shaker at 37°C for the duration of the assay (up to 6 h). Aliquots (200 µL) of the digestion mixture were subsequently collected at regular time points into an equal volume of ice-cold stop solution, to terminate amylolysis. Microfuge tubes from each sampling occasion were then

centrifuged at 16,200 x *g* (Hareus Pico, Thermo Scientific) for 6 min to spin down any starch remnants, and the supernatant collected and frozen at -20°C for subsequent analysis. Starch hydrolysis products (reducing sugars, predominantly maltose and maltotriose) in the supernatant were quantified using a Prussian blue assay method [15], which provided reliable measurements of low concentrations of reducing sugars.

Starch digestion kinetic study of dry-milled plant tissues.

The experiment was performed on dry-milled plant tissue from chickpea and wheat with different particle sizes and therefore different ratios of surface to encapsulated starch to gain insight into the effect of tissue structure and cell encapsulation on starch digestion kinetics. Four different size fractions (median size = 1.85, 0.55, and 0.38 mm, and flour <0.21 mm) of dry-milled chickpea (3.15 g) and durum wheat (2.10 g) tissue and starch isolated from these materials were each weighed into 50 mL Falcon tubes so that each tube contained 1260 ± 2 mg starch. The sample in each tube was suspended in 30 mL PBS. All samples were then hydrothermally-processed at 100°C for 1 h 25 min with intermittent stirring, and then subjected to the amylolysis procedure described above to obtain starch digestibility profiles for each size fraction. The experiment was repeated 3 times.

Starch digestibility study of intact and homogenised plant tissues.

This experiment compared the starch digestibility of macroparticles of chickpeas and durum wheat that have been hydrothermally-treated as intact tissue, and then homogenised to provide insight into the behaviour of different tissue types and its implication for the role of cell walls as physical barriers and restrictors of starch gelatinisation.

Coarse macroparticles (median size = 1.85 mm) of chickpea (3.15 g) and durum wheat (2.10 g) were each weighed into 2 x 50 mL Falcon tubes so that all tubes contained the same amount of total starch (1260 ± 2 mg per tube). The duplicate tubes were prepared, cooked, and tested in parallel (as described below), but only one was ‘homogenised’, leaving the structure of the plant tissue macroparticles in the other tube ‘intact’. The

experiment was repeated four times, with chickpea and wheat samples tested in each experimental run using the same assay.

The chickpea samples were left to soak in 7 mL PBS at room temperature (~22 °C) overnight and then boiled for 40 min, whereas wheat was soaked at room temperature for 50 min and then boiled for 10 min. Both sample types were boiled in the soaking liquor to keep the starch concentration constant. The two different hydrothermal regimes used ensured that each material type was cooked to a texture that would be considered palatable for human consumption.

After cooking, the samples were kept at 37°C for 10 min. From each pair of tubes, the macroparticles of one tube was homogenised (see below), while the other tube was left untreated so that the macroparticles remained intact. Homogenisation was carried out using an IKA T25 Digital UltraTurrax® by immersing the UltraTurrax® probe in the tube and homogenising the content for 30 s at 16.4 x 10^3 rpm. Residual material from the UltraTurrax® probe was rinsed back into the tube with an additional 3 mL of PBS. In parallel, the same volume was also added to the 'untreated' sample tube containing the intact macroparticles.

All tubes were incubated at 37°C in a water bath for a further 5 minutes, diluted to a final total volume of 30 mL with PBS (at 37°C), and then submitted to the starch amylolysis assay procedure (described in the earlier section) to monitor starch digestion over 6 h. Digestibility curves were fitted to the data points through non-linear regression.

Digestions in a Dynamic Gastric Model (DGM) and a Static Duodenal Model (SDM). This study employed the use of physiologically-relevant digestion systems that simulate the biochemical and mechanical conditions of the GIT, including oral, gastric (DGM) and duodenal (SDM) phases.

Chickpea porridge.

Chickpea porridges were prepared from dried separated cells (that contained 48.2 g starch and 10 g moisture per 100 g of dry matter), which were either left intact, or freeze-milled to disrupt the cellular integrity. For freeze-milled cells, the dried chickpea cells were subjected to 2 x 30 min of freeze-milling at 10 cycles per second (6970D Freezer/Mill®, SPEX SamplePrep L.L.C., Stanmore, Middlesex, UK) to induce cell rupture and release intracellular starch. To prepare the porridge meals, 70 g of dried chickpea cells (either freeze-milled or intact), were soaked in 180 mL water overnight and then cooked for 20 min with the addition of another 170 mL water, following the same process as described for wheat. After cooking, the total weight of the porridge was re-adjusted to 350 g by the addition of water to make up for evaporative losses. The porridge was then digested in the DGM and SDM.

One cooked portion of chickpea porridge (~350 g) contained 35.0 g of potentially available carbohydrate (of which 34.9 g was starch and 0.1 g total sugars), 9.8 g of dietary fibre, 14.8 g of protein, and 1.7 g of lipid.

Durum wheat porridge.

The results shown in the current paper are produced from further analyses of samples and data collected from the previously published study of wheat endosperm [27]. Milled macroparticles (denoted by median sizes 0.11 mm, 0.38 mm, 1.01 mm, 1.44 mm and 1.95 mm) of durum wheat endosperm (77 g) were combined with water 150 mL and heated in a saucepan with vigorous stirring for 5 min at 85°C, after which 150 mL cold water was added and heated for a further 5 min at 85°C, then brought to boiling and allowed to continue for a further 5 min. The resulting porridge was then removed from the heat source and rested at room temperature for 15 min before use in the DGM and SDM.

One cooked portion (~377g) of durum wheat porridge contained 61.1 g of potentially available carbohydrate (of which 60.0 g was starch and 0.5 g total sugars), 4.5 g of dietary fibre, 9.4 g of protein, and 1.5 g of lipid.

Dynamic Gastric Model and Static Duodenal Model.

For the oral phase, the cooked porridge minus a 2 g weighed sub-sample (removed after cooking and used as baseline) was mixed with 20 mL distilled water, and Simulated Salivary Fluid (SSF, 10 mL containing 0.15M NaCl, 3 mM urea, pH 6.9) and 1 mL of human salivary α-amylase (HSA, 900 U, Sigma, UK, dissolved in SSF) were added. After 10 min, another 2 g sub-sample was collected to represent the effect of the simulated oral digestion phase.

For the gastric phase, the remaining mixture was added to the DGM, which was already primed with 20 mL of acidified salt solution (58 mM NaCl, 30 mM KCl, 0.5 mM $CaCl_2$, 0.864 mM NaH_2PO_4, and 10 mM HCl), to simulate the contents of the stomach in fasted humans. Physiological additions of simulated gastric secretions containing 9000 U/mL of porcine gastric pepsin and 60 U/mL of gastric lipase analogue from *Rhizopus oryzae* (Amano Enzyme Inc., Nagoya, Japan), and 0.127 mM lecithin liposomes in an acidified salt solution, occurred throughout gastric digestion. Gastric samples were ejected from the DGM every 10 min over a 60 min period.

For the duodenal phase, each gastric sample was immediately weighed, neutralised to pH 7.0 with 1 M NaOH and re-weighed. Next, 30 g of each neutralised gastric sample was transferred into individual bottles containing 3.75 mL of so-called ‘hepatic mix’ and 11.25 mL of designated ‘pancreatic mix’, and placed on an orbital shaker (170 rpm) at 37 °C to represent the duodenal digestion phase. The hepatic mix contained lecithin (6.5 mM, from Lipid Products, Surrey, UK), cholesterol (4 mM), sodium taurocholate (12.5 mM) and sodium glycodeoxycholate (12.5mM) in a salt solution of NaCl (146 mM), $CaCl_2$ (2.6 mM) and KCl (4.8 mM) and was prepared fresh for each run. The pancreatic mix contained pancreatic lipase (590 U/mL), porcine co-lipase (3.2 μg/mL), porcine trypsin (11 U/mL), bovine α-

chymotrypsin (24 U/mL), and porcine α-amylase (300 U/mL) in a solution of NaCl (125 mM), $CaCl_2$ (0.6 mM), $MgCl_2$ (0.3 mM) and $ZnSO_4$ •$7H_2O$ (4.1 μM) and was prepared fresh for each run. A representative subsample (2 g) was removed at different time points (0.2, 2, 5, 10, 15, 20, 30, 40, 60, 90, 180 and 210 min) and added to ethanol (8 mL) for subsequent analysis of starch digestion products (total reducing sugars).

Overall, 1 x cooked sample, 1 x orally processed sample, 6 x gastric samples, and 72 (i.e. 6 x 12) duodenal samples were collected per run. Two runs were performed with intact cells and one run performed with freeze-milled samples, and all analysis was performed in triplicate. Additional samples for microscopy analysis were collected at key time points and immediately immersed into Karnovsky's fixative and later processed and embedded in LR resin as described (see *'Light microscopy').* Samples for analysis of dry matter were frozen (-20 °C) in plastic pots and determined by oven-drying at 102°C.

Samples collected into ethanol for analysis of starch digestion were stored at 4°C and centrifuged at 4000 x g for 2 min prior to reducing sugar analysis. For the chickpea study, reducing sugar concentration was determined by DNS assay as described elsewhere [10], whereas analysis of starch digestion products from durum wheat porridge was performed at Quadram Institute Bioscience (formerly Institute of Food Research, Norwich) as described previously [27]. The different reducing sugar assay methods used have been compared previously [28,29] and were selected based on the suitability of the working range and compatibility with samples obtained from these studies.

Data and Statistical analysis.

Graphing, curve-fitting and statistical analyses were performed in GraphPad Prism (version 8.4.3, Graph Pad software, San Diago, CA, USA). Comparison of time-course data was performed by One-way ANOVA or mixed effects model with Tukey's correction for multiple comparisons or by paired t-test, as indicated in figure legends. Tukey's *post-hoc* test was applied when there was a significant effect of treatment. Statistically significant differences

were accepted at $p < 0.05$. A paired t-test was used when only two curves where compared. Non-linear regression analysis was applied to time-course data by least squares regression to a one or two-phase association equation, and 95% confidence bands obtained to show likely location of the true curve.

Acknowledgements

We thank RHM Analytical Services (Premier Foods) for proximate analysis data on the wheat and chickpea samples; G. Campbell, and S. Galindez-Najera (at the University of Manchester) for technical expertise, assistance and use of facilities for preparation of the milled materials, G. Vizcay-Barrena from the Centre for Ultra-structural Imaging at King's College for sectioning microscopy samples and the Model Gut team at the Institute of Food Research for use of the gastric and duodenal digestion models (DGM and SDM).

This project was funded by the Biotechnology and Biological Sciences Research Council (BBSRC), UK, DRINC BB/H004866/1 and C.H.E. was in receipt of a BBSRC CASE studentship award with Premier Foods (UK) as an industrial partner. Edwards gratefully acknowledges the support of BBSRC Institute Strategic Programme Food Innovation and Health BB/R012512/1 and its constituent project BBS/E/F/000PR10345.

Author Contributions

C.E., P.E., G.M. and P.B. designed the research; C.E. conducted the research; C.E., P.R, G.M., P.E. and P.B. analysed the data; C.E. wrote the paper, and P.R., G.M. and P.B. contributed to revisions of the manuscript. P.E. had primary responsibility for final content. All authors read and approved the final manuscript.

Competing Interests

CH Edwards, P Ryden, G Mandalari, PR Ellis and PJ Butterworth declare no competing interests.

Data Availability

Source data for curves fitted in figure(s) 1, 3, 4 and 5 are provided with the paper, and the other datasets generated during and/or analysed during the current study are available from the corresponding author on reasonable request.

Supplementary Information

Supplementary Figure 1. Effect of gastric residence time on duodenal digestion of chickpea porridges.

Supplementary Figure 2. Effect of gastric residence time on duodenal digestion of durum wheat porridges.

References

1 Stephen, A. M. et al. Dietary fibre in Europe: current state of knowledge on definitions, sources, recommendations, intakes and relationships to health. *Nutr. Res. Rev*. **30**, 149-190, doi: https://doi.org/10.1017/s095442241700004x (2017).

2 Grundy, M. M.-L. et al. Re-evaluation of the mechanisms of dietary fibre and implications for macronutrient bioaccessibility, digestion and postprandial metabolism. *Brit. J. Nutr*. **116**, 816-833, doi: https://doi.org/10.1017/S0007114516002610 (2016).

3 Jarvis, M. C., Briggs, S. P. H. & Knox, J. P. Intercellular adhesion and cell separation in plants. *Plant Cell Environ*. **26**, 977-989, doi: https://doi.org/10.1046/j.1365-3040.2003.01034.x (2003).

4 Golay, A. et al. Comparison of metabolic effects of white beans processed into 2 different physical forms. *Diabetes Care* **9**, 260-266, doi: https://doi.org/10.2337/diacare.9.3.260 (1986).

5 Chu, J., Ho, P. & Orfila, C. Growth region impacts cell wall properties and Hard-to-Cook phenotype of canned navy beans (Phaseolus vulgaris). *Int. J. Food Process Technol*. **13**, 818-826, doi: https://doi.org/10.1007/s11947-020-02436-7 (2020).

6 Pallares Pallares, A., Loosveldt, B., Karimi, S. N., Hendrickx, M. & Grauwet, T. Effect of process-induced common bean hardness on structural properties of in vivo generated boluses and consequences for in vitro starch digestion kinetics. *Brit. J. Nutr*. **122**, 388-399, doi: https://doi.org/10.1017/s0007114519001624 (2019).

7 Noah, L. et al. Digestion of carbohydrate from white beans (Phaseolus vulgaris L.) in healthy humans. *J. Nutr*. **128**, 977-985, doi: https://doi.org/10.1093/jn/128.6.977 (1998).

8 Petropoulou, K. et al. A natural mutation in Pisum sativum L. (pea) alters starch assembly and improves glucose homeostasis in humans. *Nature Food*, doi: https://doi.org/10.1038/s43016-020-00159-8 (2020).

9 Grassby, T. et al. Modelling of nutrient bioaccessibility in almond seeds based on the fracture properties of their cell walls. *Food Funct*. **5**, 3096-3106, doi: https://doi.org/10.1039/C4FO00659C (2014).

10 Edwards, C. H. et al. Manipulation of starch bioaccessibility in wheat endosperm to regulate starch digestion, postprandial glycemia, insulinemia, and gut hormone responses: a randomized controlled trial in healthy ileostomy participants. *Am. J. Clin. Nutr*. **102**, 791-800, doi: https://doi.org/10.3945/ajcn.114.106203 (2015).

11 Würsch, P., Del Vedovo, S. & Koellreutter, B. Cell structure and starch nature as key determinants of the digestion rate of starch in legume. *Am. J. Clin. Nutr*. **43**, 25-29, doi: https://doi.org/10.1093/ajcn/43.1.25 (1986).

12 Dhital, S., Bhattarai, R. R., Gorham, J. & Gidley, M. J. Intactness of cell wall structure controls the in vitro digestion of starch in legumes. *Food Funct*. **7,** 1367-1379, doi: https://doi.org/10.1039/C5FO01104C (2016).

13 Rovalino-Córdova, A. M., Fogliano, V. & Capuano, E. The effect of cell wall encapsulation on macronutrients digestion: A case study in kidney beans. *Food Chem*. **286,** 557-566, doi: https://doi.org/10.1016/j.foodchem.2019.02.057 (2019).

14 Edwards, C. H., Maillot, M., Parker, R. & Warren, F. J. A comparison of the kinetics of in vitro starch digestion in smooth and wrinkled peas by porcine pancreatic alpha-amylase. *Food Chem*. **244,** 386-393, doi: https://doi.org/10.1016/j.foodchem.2017.10.042 (2018).

15 Edwards, C. H., Warren, F. J., Milligan, P. J., Butterworth, P. J. & Ellis, P. R. A novel method for classifying starch digestion by modelling the amylolysis of plant foods using first-order enzyme kinetic principles. *Food Funct*. **5**, 2751-2758, doi: https://doi.org/10.1039/C4FO00115J (2014).

16 Al-Rabadi, G. J. S., Gilbert, R. G. & Gidley, M. J. Effect of particle size on kinetics of starch digestion in milled barley and sorghum grains by porcine alpha-amylase. *J. Cereal Sci.* **50,** 198-204, doi: https://doi.org/10.1016/j.jcs.2009.05.001 (2009).

17 Korompokis, K., De Brier, N. & Delcour, J. A. Differences in endosperm cell wall integrity in wheat (Triticum aestivum L.) milling fractions impact on the way starch responds to gelatinization and pasting treatments and its subsequent enzymatic in vitro digestibility. *Food Fun*ct. **10**, 4674-4684, doi: https://doi.org/10.1039/C9FO00947G (2019).

18 Rovalino-Córdova, A. M., Fogliano, V. & Capuano, E. A closer look to cell structural barriers affecting starch digestibility in beans. *Carbohydr. Polym*. **181**, 994-1002, doi: https://doi.org/10.1016/j.carbpol.2017.11.050 (2018).

19 Edwards, C. H. et al. A study of starch gelatinisation behaviour in hydrothermally-processed plant food tissues and implications for in vitro digestibility. *Food Funct*. **6**, 3634-3641, doi: https://doi.org/10.1039/C5FO00754B (2015).

20 Pitino, I. et al. Survival of Lactobacillus rhamnosus strains in the upper gastrointestinal tract. *Food Microbiol*. **27,** 1121-1127, doi: https://doi.org/10.1016/j.fm.2010.07.019 (2010).

21 Vardakou, M. et al. Achieving antral grinding forces in biorelevant in vitro models: Comparing the USP Dissolution Apparatus II and the Dynamic Gastric Model with human In vivo data. *AAPS PharmSciTech*. **12**, 620-626, doi: https://doi.org/10.1208/s12249-011-9616-z (2011).

22 Bhattarai, R. R., Dhital, S., Wu, P., Chen, X. D. & Gidley, M. J. Digestion of isolated legume cells in a stomach-duodenum model: three mechanisms limit starch and protein hydrolysis. *Food Funct*. **8**, 2573-2582, doi: https://doi.org/10.1039/C7FO00086C (2017).

23 Pallares Pallares, A. et al. Process-induced cell wall permeability modulates the in vitro starch digestion kinetics of common bean cotyledon cells. *Food Funct*. **9**, 6544-6554, doi: https://doi.org/10.1039/C8FO01619D (2018).

24 Wood, J. A. et al. Genetic and environmental factors contribute to variation in cell wall composition in mature desi chickpea (Cicer arietinum L.) cotyledons. *Plant Cell Environ*. **41**, 2195-2208, doi: https://doi.org/10.1111/pce.13196 (2018).

25 Edwards, C. H., Cochetel, N., Setterfield, L., Perez-Moral, N. & Warren, F. J. A single-enzyme system for starch digestibility screening and its relevance to understanding and predicting the glycaemic index of food products. *Food Funct*. **10**, 4751-4760 doi: https://doi.org/10.1039/C9FO00603F (2019).

26 Goñi, I., Garcia-Alonso, A. & Saura-Calixto, F. A starch hydrolysis procedure to estimate glycemic index. *Nutr. Res*. **17**, 427-437, doi: https://doi.org/10.1016/S0271-5317(97)00010-9 (1997).

27 Mandalari, G. et al. Durum wheat particle size affects starch and protein digestion in vitro. *Eur. J. Nutr*. **57**, 319-325, doi: https://doi.org/10.1007/s00394-016-1321-y (2018).

28 Slaughter, S. L., Ellis, P. R., Jackson, E. C. & Butterworth, P. J. The effect of guar galactomannan and water availability during hydrothermal processing on the hydrolysis of starch catalysed by pancreatic alpha-amylase. *Biochim. Biophys. Acta* **1571**, 55-63, doi: https://doi.org/10.1016/S0304-4165(02)00209-X (2002).

29 Hussain, H., Ngaini, Z. & Chong, N. F.-M. Modified bicinchoninic acid assay for accurate determination of variable length reducing sugars in carbohydrates. *Int. Food Res. J*. **25**, 2614-2619 (2018).

Figure Legends

Figure 1 Particle size and starch digestion kinetics. The effect of dry-milled particle size on starch digestibility in hydrothermally-cooked chickpea (**a**) and durum wheat (**b**) was investigated in chickpea cotyledon and durum wheat endosperm tissue particles and in starch extracted from these tissues. All samples were dry-milled and sieved to obtain distinct size fractions, then hydrothermally-processed at 100°C for 1 h 25 min before incubation with pancreatic α-amylase (~0.17 U per mg starch). Starch amylolysis products were quantified by Prussian blue assay and expressed as maltose-equivalents. The concentration of reducing sugars before the addition of pancreatic amylase was negligible. The legend indicates median particle size and different superscript letters indicate a significant difference in starch digestibility between particle size fractions within chickpea or durum wheat ($p < 0.05$, mixed-effects model ANOVA with Tukey's *post-hoc* test). Values are mean of triplicates; error bars are SEM. Curves were obtained by least squares regression to two-phase association equations and 95% confidence bands show the likely location of the true curve. R^2 >0.99 for all curves.

Figure 2 Microstructure of hydrothermally-cooked intact tissue macroparticles. Cross-sections of chickpea (left, **a,c,e**) and wheat (right, **b,d,f**), before (**a,b**), and after (**c,d,e,f**) digestion. Light micrographs of cross-sections of chickpea (left, **a,c,e**) and wheat (right, **b,d,f**) cut to 0.5 µm thickness and stained with toluidine blue (1% w/v, with 1% w/v sodium borate). Scalebar = 50 µm. In micrographs captured before digestion (**a,b**), the cell walls are seen to surround intracellular starch within the intact tissue, with some ruptured ('RC') and/or empty ('EC') cells present on the particle edges (i.e., the fractured surface created by dry-milling). Arrows indicate some of the areas where weakening of inter-cellular linkages has occurred. The internal structure and edges of chickpea tissue examined after 4 h of *in vitro* digestion (**c**) did not appear to be altered. After 2 h digestion, wheat starch was still evident within many endosperm cells, particularly those in close proximity to the aleurone layer or crease (**d**). The appearance of chickpea tissue remained unchanged after 6 h (**e**), whereas wheat endosperm cells near the particle edges had collapsed and/or had been eroded ('edge') after 6 h (**f**).

Figure 3 Homogenisation of cooked macroparticles and starch digestibility. Light micrographs of homogenised macroparticles of chickpea (left) and wheat (right) captured before (**a,b**) and after 6 h (**c,d**) *in vitro* digestion, stained with 2.5% Lugol's iodine solution. Scalebar = 50 µm. Intact macroparticles (1.85 mm) of chickpea and durum wheat endosperm were hydrothermally-cooked prior to homogenisation by UltraTurrax® for 30 s at 16.4 x 10^3 rpm. Homogenisation caused cell separation in chickpea (**a**) and cell rupture in wheat (**b**). After 6 h incubation with amylase, the chickpea cells remained intact (**c**) while starch granules released from cells by homogenisation pre-treatment had been digested (**c,d**). Starch digestibility curves show the progress of starch digestion of hydrothermally-cooked intact and homogenised macroparticles of chickpea (**e**) and wheat (**f**). The digestions were performed in quadruplicate, and values are means with error bars as SEM. Significant

differences between starch digestion from intact and homogenised particles are indicated (paired t-test), $^{**}p < 0.01$, $^{***}p < 0.001$, and 'ns' not significant, $p > 0.05$. Curves were obtained by least squares regression to two-phase association equations and 95% confidence bands show the likely location of the true curve. R^2 values were 0.95 and 0.92 for intact and homogenised chickpea, and 0.98 and 0.81 for intact and homogenised durum wheat, respectively.

Figure 4: Gastric and duodenal digestion of chickpea porridges with contrasting cell structure. Chickpea porridges made with intact or freeze-milled chickpea cells were digested using a dynamic gastric model followed by a static duodenal model. Starch digestibility curves show the percentage of total starch that has been digested at each time point from chickpea porridge made from intact or freeze-milled cells in the stomach (**a**) and duodenum (**b**). Profiles shown in panel **b** and **c** are of samples subjected to 60 min gastric residence, wherein the gastric baseline has been subtracted (**b**), or included to give the total amount of starch amylolysis (**c**). Curve fits were obtained by least square regression to one (**a**, $R^2 > 0.99$) or two (**b**, $R^2 > 0.99$) -phase association equations, with 95% confidence bands shown. (**d**) Micrographs of intact (**d1,d3**), and freeze-milled (**d2,d4**) porridge captured before (**d1,d2**) and after (**d3,d4**) duodenal digestion. All stained with KI, scalebar = 100 μm. All experimental points are the mean of three determinations obtained from one (freeze-milled) or two (intact) simulated digestion runs and the error bars show 20% standard error. (**e**) Clustered column chart showing percentage of total starch that has been digested at the end of duodenal phase, clustered by cell treatment type (intact versus freeze-milled) and with a separate column shown for each gastric residence time. The overlaid columns with a dark border represent the extent of starch released from each sample during the gastric phase.

Figure 5: Gastric and duodenal digestion of wheat porridges with contrasting particle size. Wheat porridges made with different particle size fractions of milled endosperm were digested using a dynamic gastric model followed by a static duodenal model. Starch digestibility curves show the percent of total starch that has been digested at each time point from wheat endosperm porridge with contrasting particle sizes in the stomach (**a**) and duodenum (**b**). Profiles shown in panel **b** and **c** are of samples subjected to 60 min gastric residence, wherein the gastric baseline has been subtracted (**b**), or included to give the total amount of starch amylolysis (**c**). Curve fits were obtained by least square regression to one (**a**, $R^2 > 0.98$) or two (**b**, $R^2 > 0.99$) - phase association equations, with 95% confidence bands shown. (**d**) Micrographs of particle size 0.11 mm (**d1,d4**), 1.01 mm (**d2,d5**) and 1.95 mm (**d3,d6**) captured before (**d1,d2**), mid-gastric (**d3**) and after duodenal digestion (**d4,d5,d6**), were all stained with KI, scalebar = 100 μm. (**e**) Clustered column chart showing % of total starch that has been digested at the end of duodenal phase, clustered by particle size and with a separate column shown for each gastric residence time (10-60 min). All experimental points are the mean of three determinations obtained from three simulated digestion runs and the error bars show 20% standard error. The overlaid columns with a dark border represent the starch released from each sample during the gastric phase.

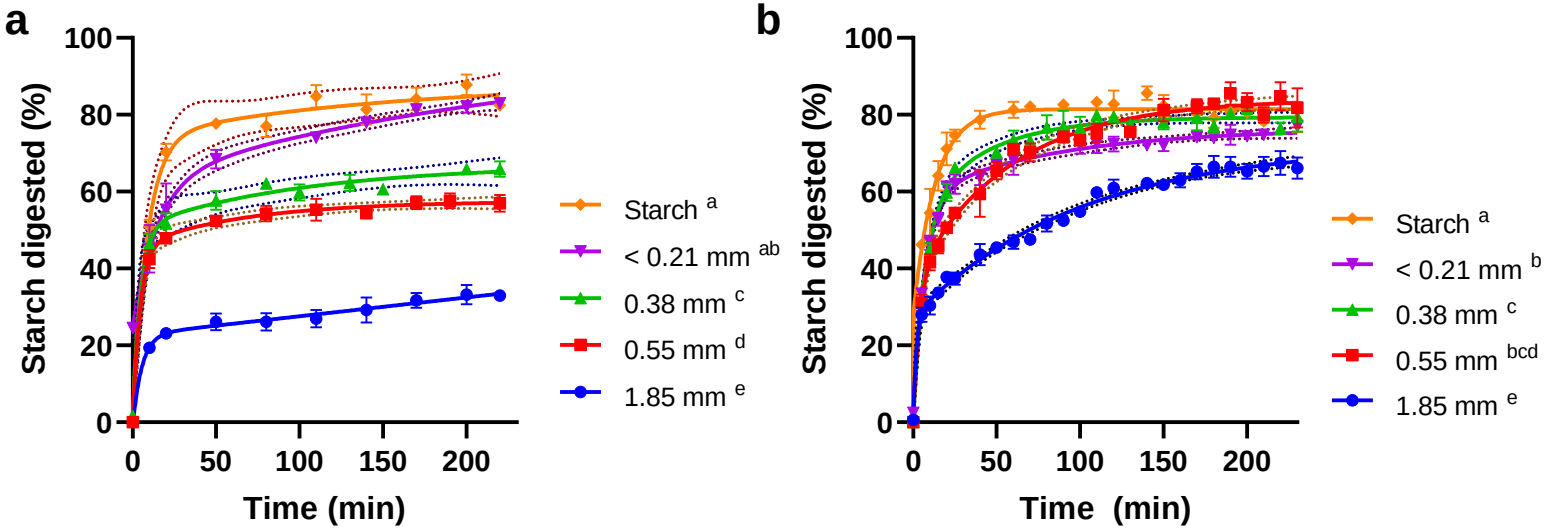
a
Starch digested (%)
Time (min)
Starch a
< 0.21 mm ab
0.38 mm c
0.55 mm d
1.85 mm e
b
Starch digested (%)
Time (min)
Starch a
< 0.21 mm b
0.38 mm c
0.55 mm bcd
1.85 mm e

a

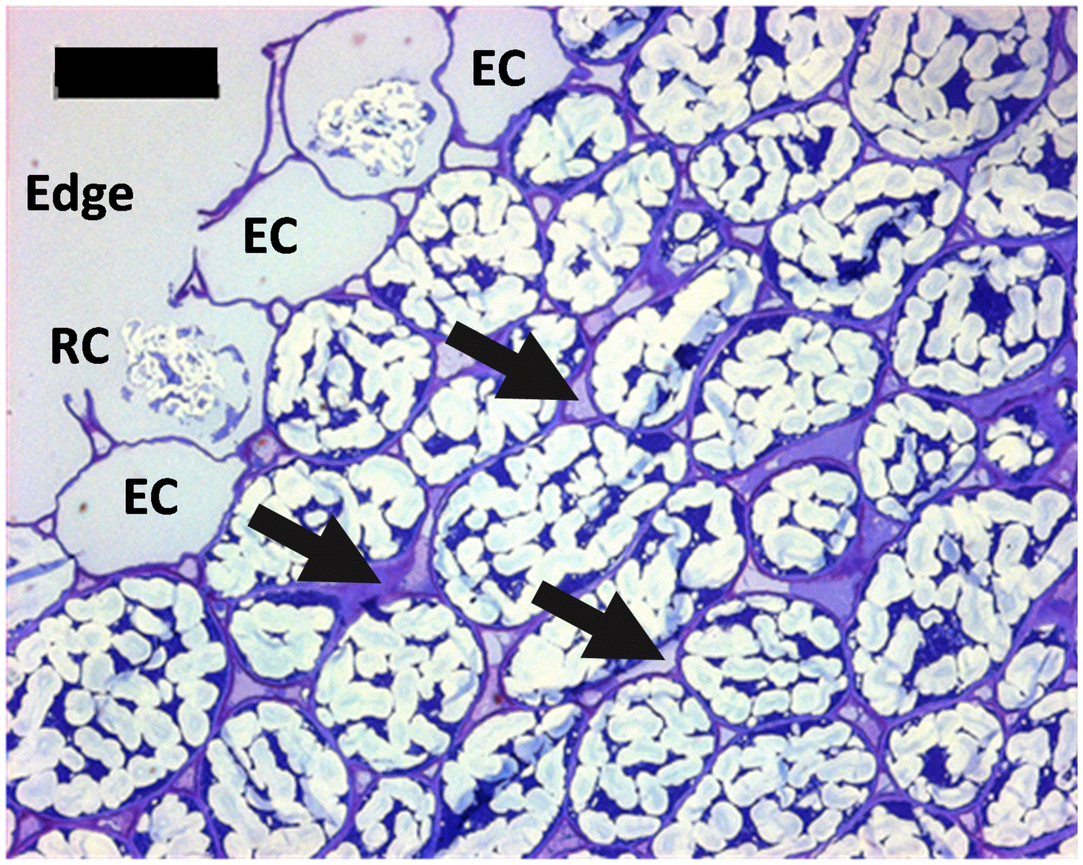

b

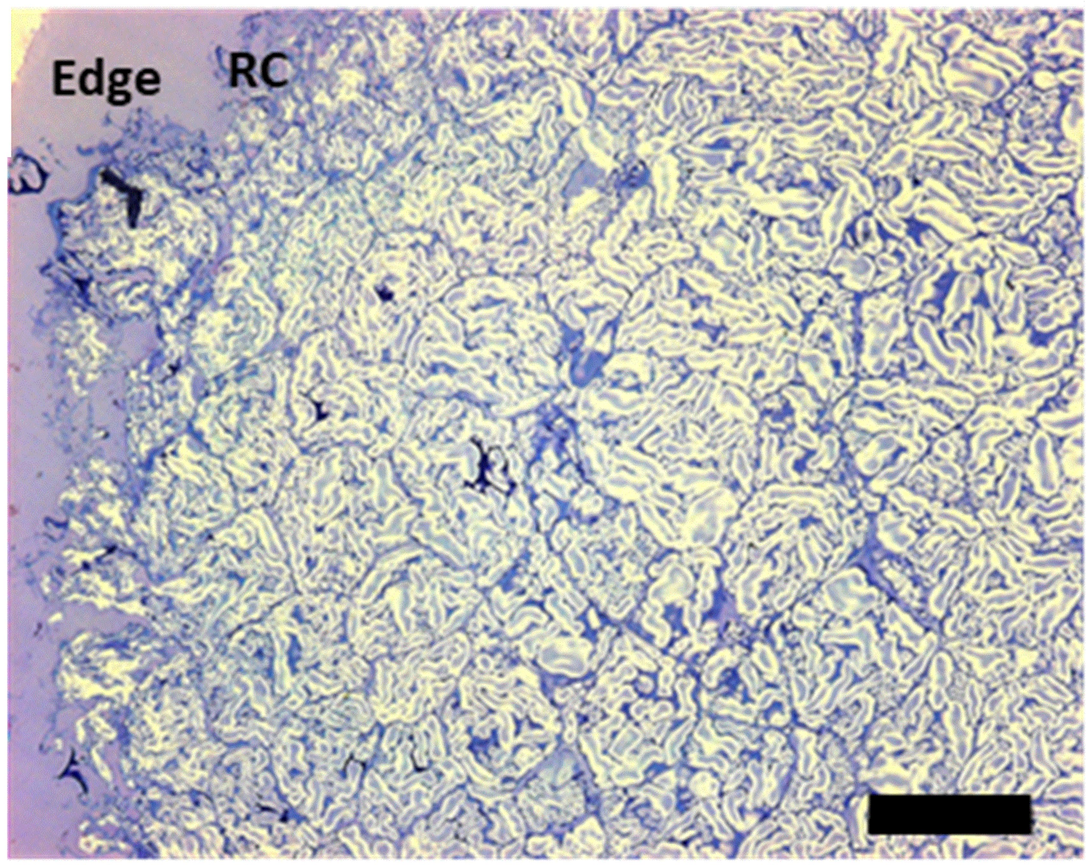

c

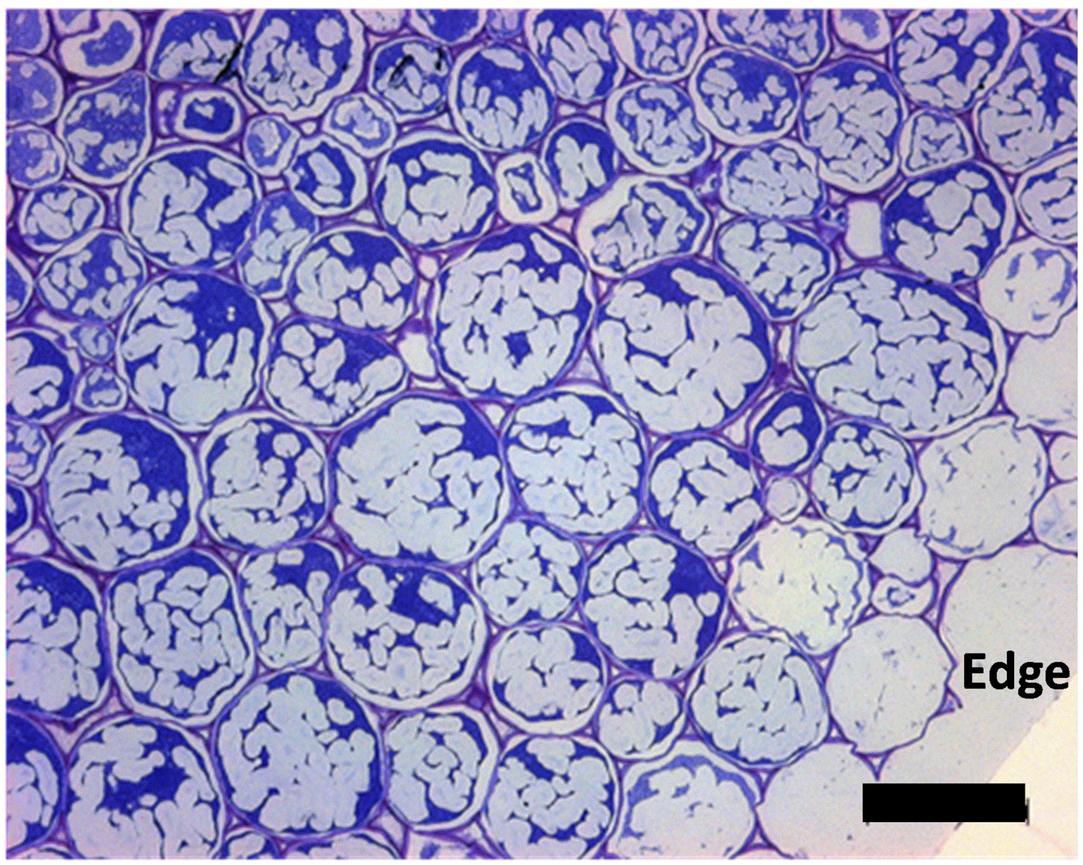

d

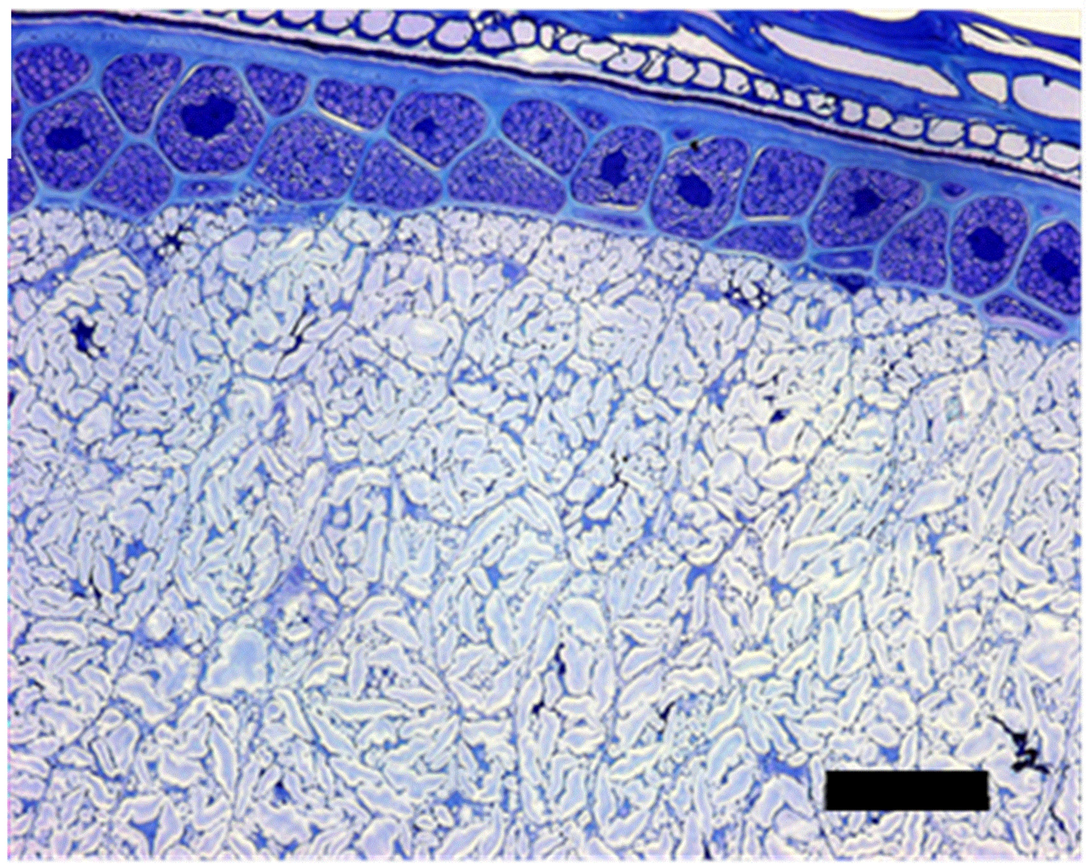

e

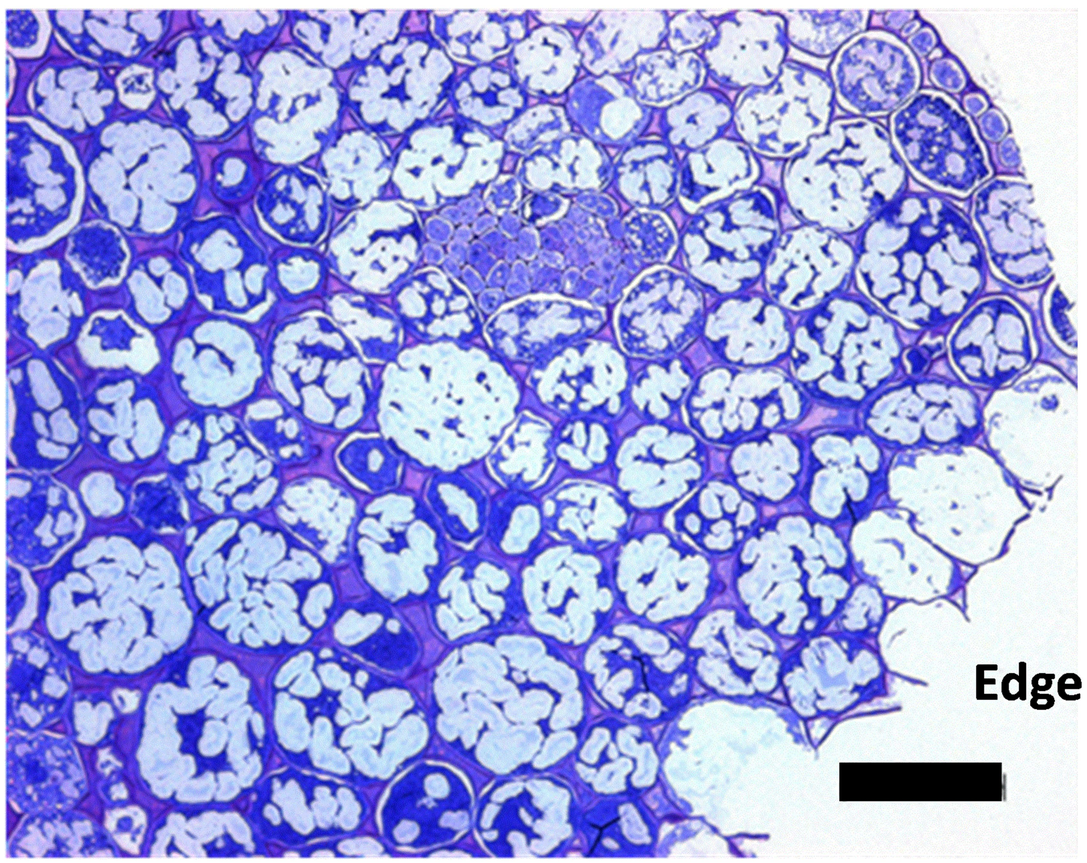

f

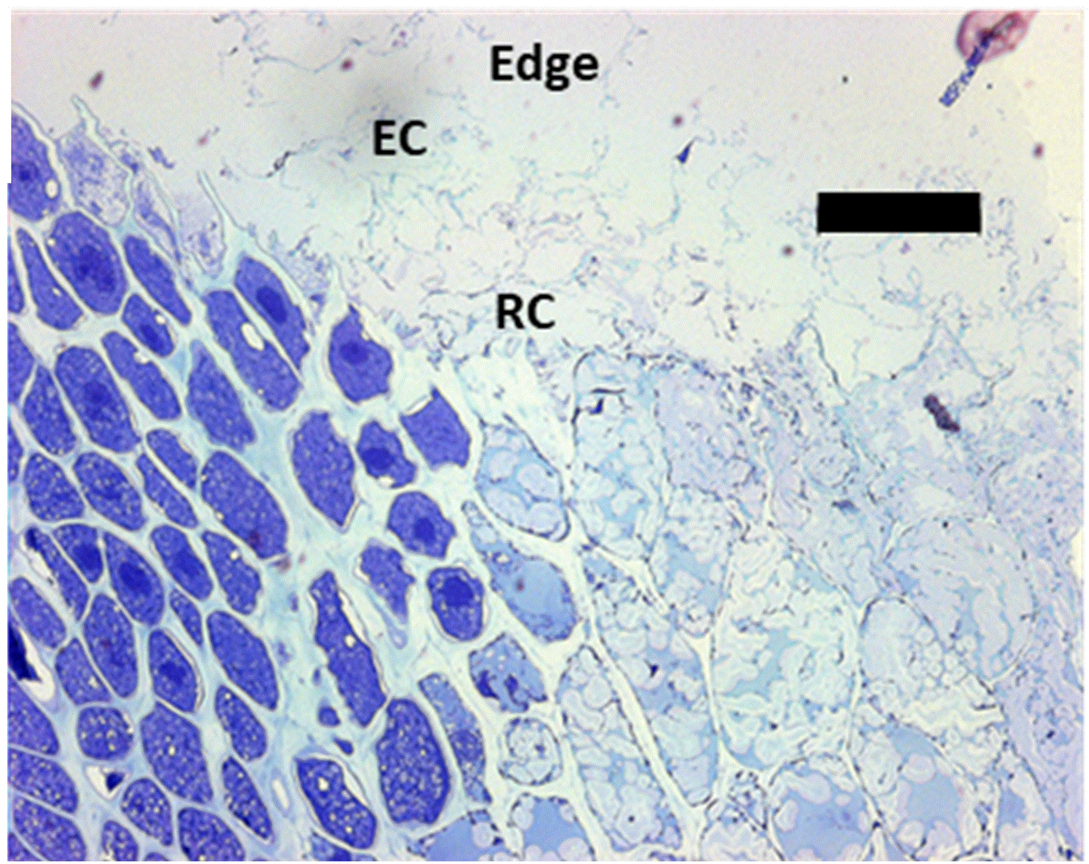

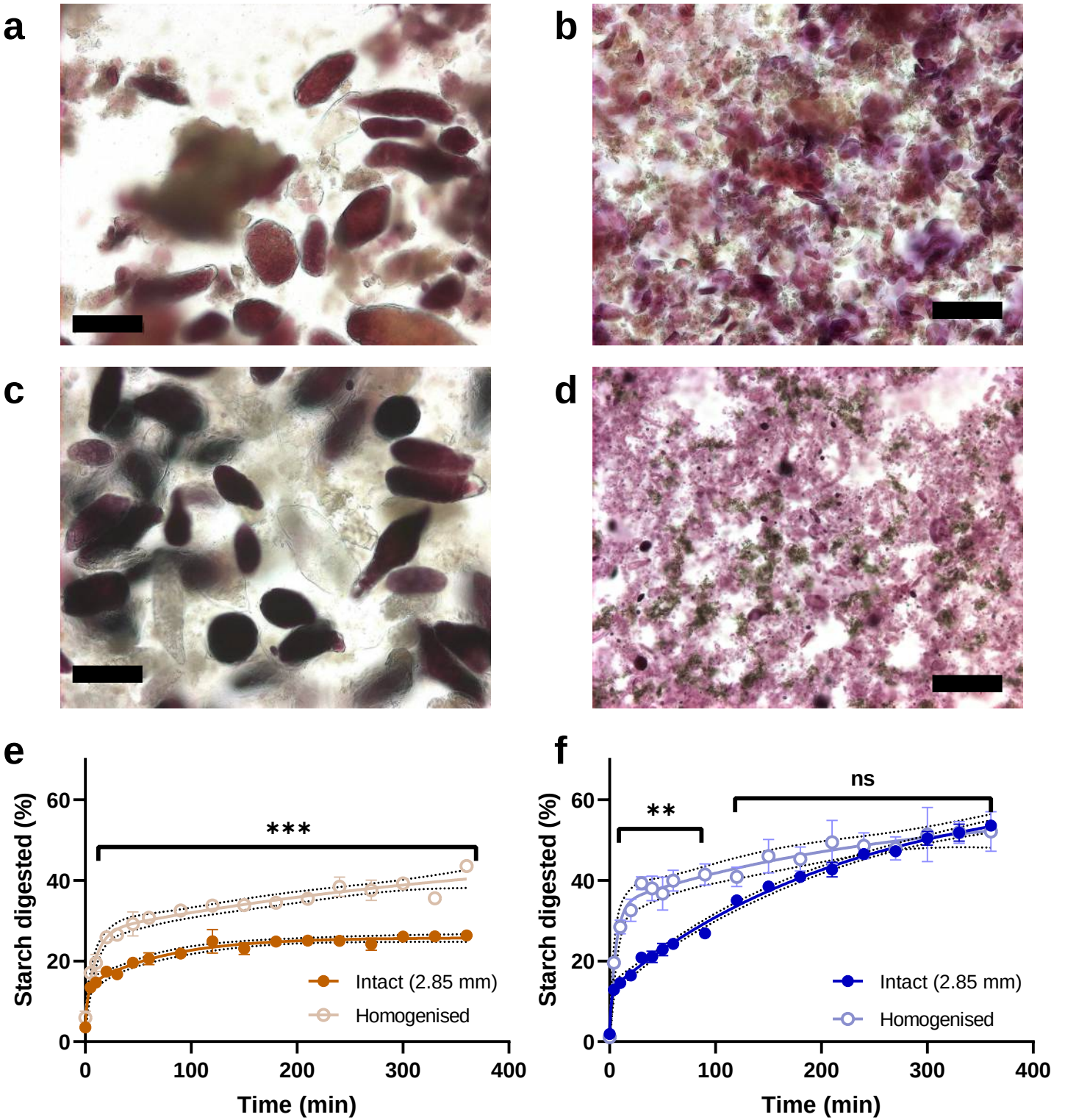
a
b
c
d
e
f
Starch digested (%)
Time (min)
***
Intact (2.85 mm)
Homogenised
**
ns

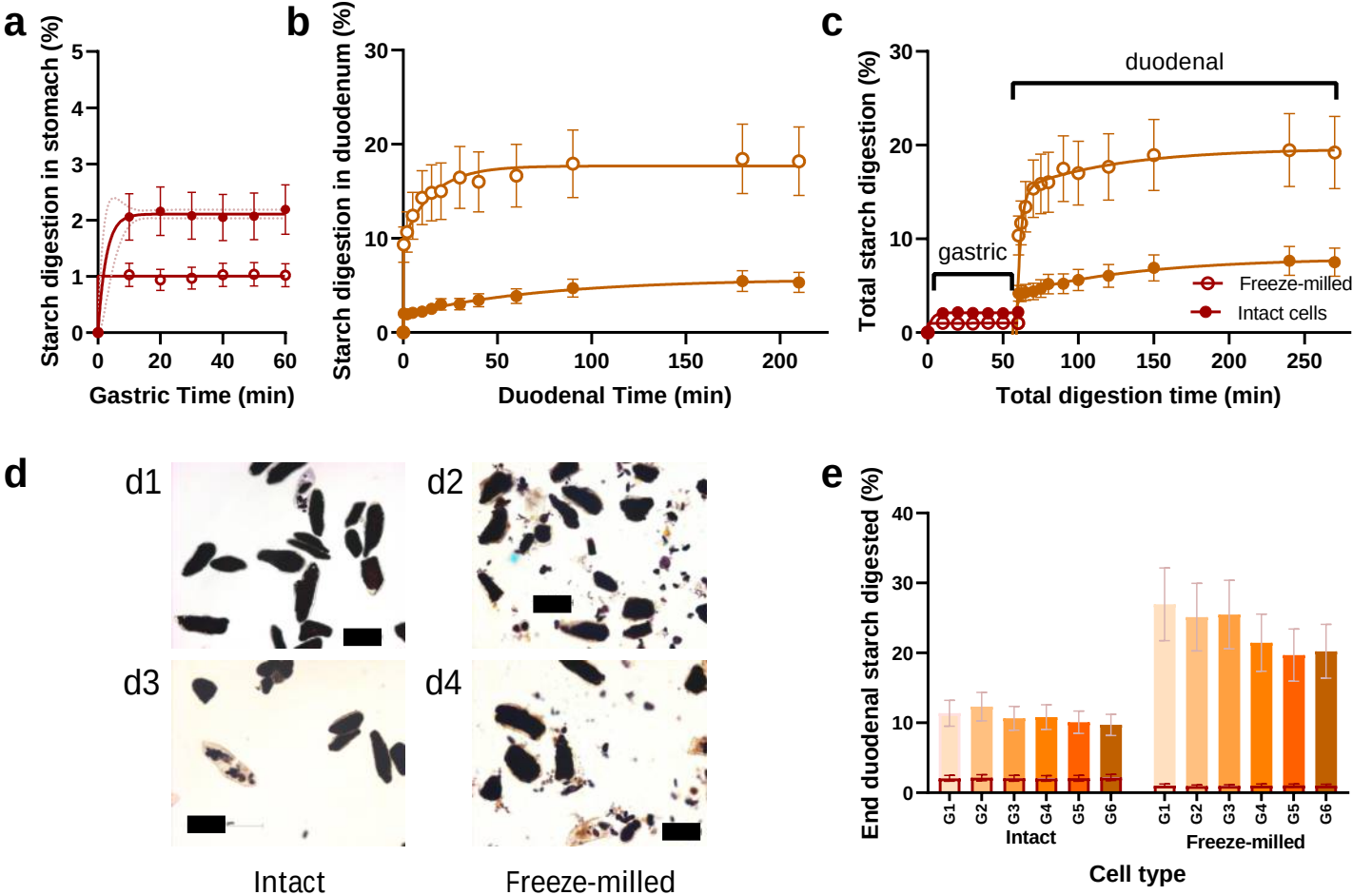
a
Starch digestion in stomach (%)
Gastric Time (min)
b
Starch digestion in duodenum (%)
Duodenal Time (min)
c
Total starch digestion (%)
duodenal
gastric
Freeze-milled
Intact cells
Total digestion time (min)
d
d1
d2
d3
d4
Intact
Freeze-milled
e
End duodenal starch digested (%)
G1
G2
G3
G4
G5
G6
Intact
Freeze-milled
Cell type

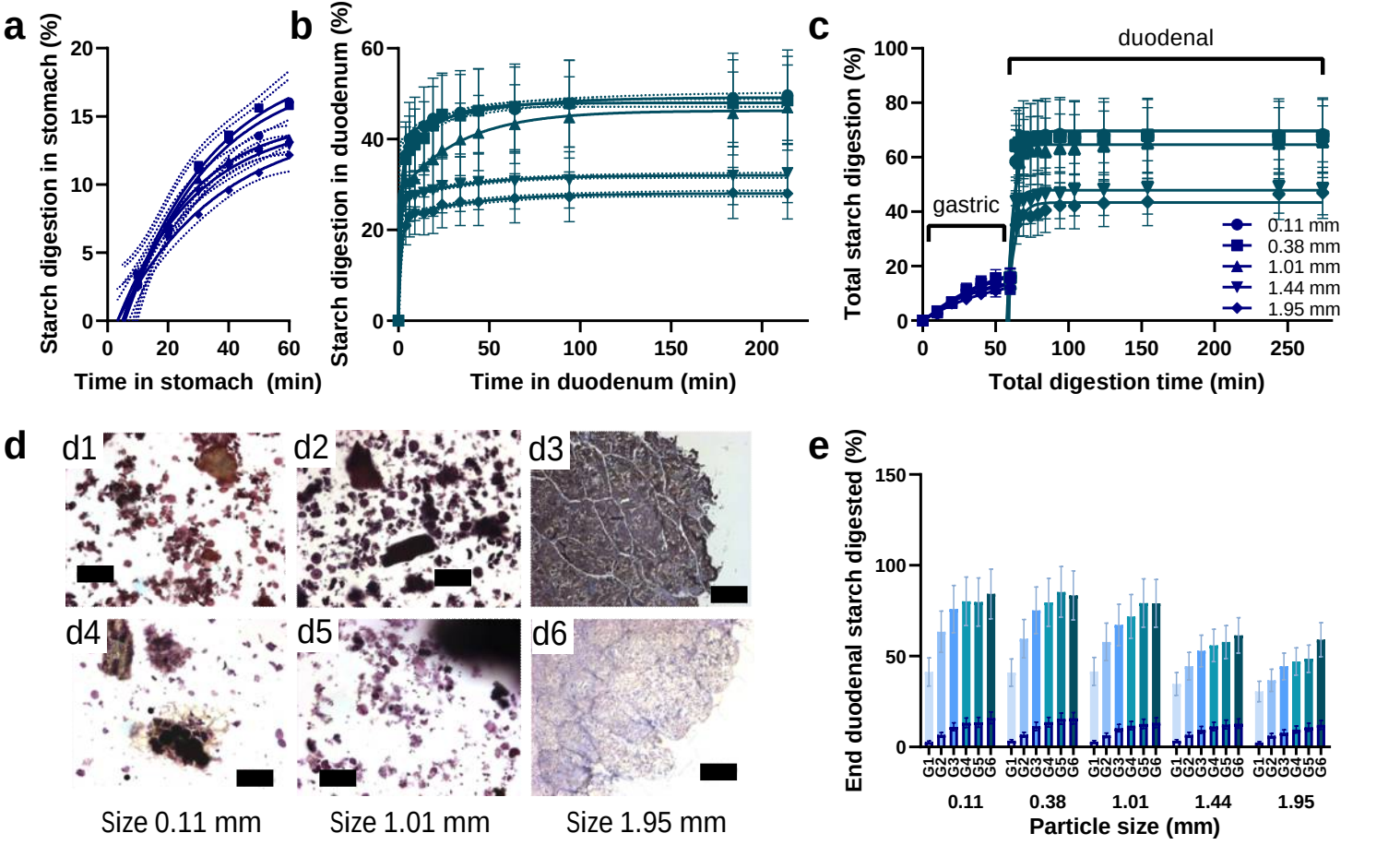
a
Starch digestion in stomach (%)
Time in stomach (min)
b
Starch digestion in duodenum (%)
Time in duodenum (min)
c
duodenal
gastric
Total starch digestion (%)
Total digestion time (min)
0.11 mm
0.38 mm
1.01 mm
1.44 mm
1.95 mm
d
d1
d2
d3
d4
d5
d6
Size 0.11 mm
Size 1.01 mm
Size 1.95 mm
e
End duodenal starch digested (%)
Particle size (mm)
0.11
0.38
1.01
1.44
1.95